

Minimization of the Fading Effect in Indoor Wireless Communication using Coherent 16-Amplitude Phase Shift Keying with Regular Low Density Parity Check Code

Wei Wei¹ & Junghwan Kim²

Abstract

Signal degradation in indoor wireless communication systems is often occurred because of random changes in attenuation within the transmission medium. Such signal perturbations are referred to as fading and it may affect the bit error probability (BEP) performance of the system tremendously. To alleviate this degradation, we propose a system, regular low density parity check (LDPC) coded 16-ary amplitude phase shift keying (16-APSK) with coherent detection assuming the four-ray Rayleigh fading model as well as the effect of delay spread. Simulation results assert that with the aid of regular LDPC code, the effect of fading has been considerably mitigated, thus the proposed system could easily approach the expedient BEP. Further results of BEP comparisons are also provided between the proposed system and the conventional three-ray fading model.

Keywords: BEP, 16-APSK with coherent detection, 4-ray Rayleigh fading model, indoor wireless communications, multipath signals, regular LDPC code.

1. Introduction

In indoor wireless communication systems, such as device-to-device (D2D) communications, transmitted signals may be scattered by surrounding objects that can lead to the signal fading because each transmission signal goes through different paths [1-2]. This causes both the constructive and destructive interference that affect the BEP performance at large. In the previous works, the spread spectrum techniques [15-16] was utilized to alleviate the problem of the fading resulted from multipath due to its processing gain (PG). This factor is the ratio of bit duration of information-bearing signal to chip duration of spreading code. Accordingly, by increasing the PG, the BEP degradation due to fading can be compensated, but it requires extra bandwidth [29] for efficient data transmission.

To mitigate the effect of channel fading without using spread spectrum techniques, we utilize regular LDPC code [3] that employs iterative decoding algorithm. Since the BEP performance of one communication system is also affected by the proper selection of modulation schemes, 16-APSK [4] is selected with coherent detection to maintain the expected BEP performance instead of non-coherent systems, while sufficient bandwidth efficiency is maintained by using bits per symbol. The contribution of this work can be summarized as follows:

- (a) The analytic form of the BEP of the proposed scheme over the AWGN and multipath fading channel are derived and analyzed.
- (b) By using the measurement data [1], the BEP performance of the proposed system at $f = 2.5$ GHz is evaluated, which can be used widely in practical indoor wireless communications.
- (c) Both the multiple ray fading models (4 rays) and practical delay spread are discussed and effects of them are evaluated through the BEP performance analysis.
- (d) For the proposed coded system, results of BEP comparison are provided both for the 4-ray and the conventional three-ray model fading.

¹Ph. D. student, Department of Electrical Engineering and Computer Science, The University of Toledo, Toledo, OH, U.S.A. E-mail: wei.wei@rockets.utoledo.edu

²Professor, Department of Electrical Engineering and Computer Science, The University of Toledo, Toledo, OH, U.S.A. E-mail: jung.kim@utoledo.edu

The remainder of this paper is organized as follows. The proposed coded system model is defined and described in Section 2. Section 3 describes on the coherent 16-APSK and the regular LDPC code is discussed in Section 4. Aspect of the delay spread is discussed in Section 5. Discussion on the results of computer simulations can be found in the last section of this paper along with the conclusion.

2. Proposed Coded 16-APSK Indoor Wireless System Model

Fig. 1 shows the block diagram of the signal flow in the proposed system model. At the transmitter, the binary data sequence is encoded by regular LDPC encoder and is modulated by 16-APSK modulator and transmitted through 4-ray Rayleigh fading channel. To evaluate the BEP under practical Rayleigh fading effect at least three rays [25-27] needs to be emulated for the multipath propagation. Instead, we utilize four-ray model to possibly yield better signal detection than the conventional three-ray model with larger constructive received power. At the receiver, carriers are removed by coherent 16-APSK demodulator and decoded by regular LDPC decoder towards the final output data.

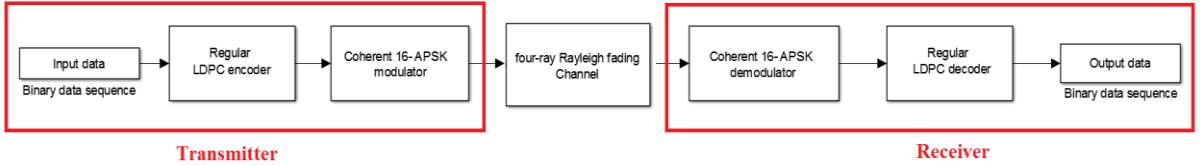


Fig. 1. Signal flow of the coded 16-APSK indoor wireless communication system under four-ray Rayleigh fading

For the evaluation of the error performance of the considered indoor wireless communication system centered at $f = 2.5$ GHz, we modified the three-ray Rayleigh fading model of [1] as in Fig. 2. In general, the received signal at the receiver is considered as the result of multipath propagation [28]. Accordingly, in this paper, the signal route via object 1 is referred to as one-ray model with the reflected ray V_1 , and three-ray model refers to the signal routes scattered via objects 1, 2 and 3 with the reflected ray V_1 , V_2 and V_3 respectively. In addition, all signal paths from the transmitter to the receiver will be referred to as the proposed four-ray model with all four reflected rays. Note that each reflected ray can be represented by $A \cos(\omega t - \theta)$ [28]. According to Lambert's cosine law [33], the range of A is between 0 and 1. When the reflected angle is approached 0° , A is approached 1. As a result, A of reflected ray V_1 , V_2 , V_3 , and V_4 can be selected as 0.5, 0.33, 0.66 and 0.85 [28]. Finally, θ is related to the effect of delay spread [28] and its value is usually extreme small with center frequency at $f = 2.5$ GHz [1]. Hence, θ can be 0° for simplicity with $\omega = 2\pi f$.

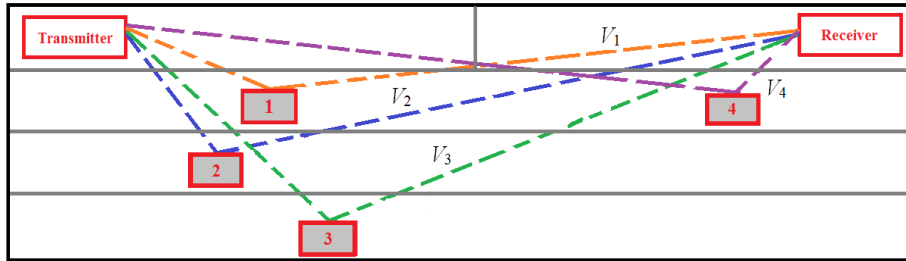


Fig. 2. Proposed 4 rays rack-to-rack Rayleigh fading model used in indoor wireless communications.

3. 16-APSK with Coherent Detection

It is well known that the most significant advantage of 16-APSK with coherent detection is to have lower peak-to-average power ratio (PAPR) along with better BEP performance if used in multi-carrier system such as orthogonal frequency division multiple (OFDM) [31]. In addition, depending on the channel condition, APSK signal constellation can be adjustable. Hence, this paper utilizes coherent 16-APSK scheme with its circular-based constellation as illustrated in Fig. 3. Each symbol is assigned to a specific region denoted by the dotted circle and lines as their decision regions [6] for BEP performance analysis.

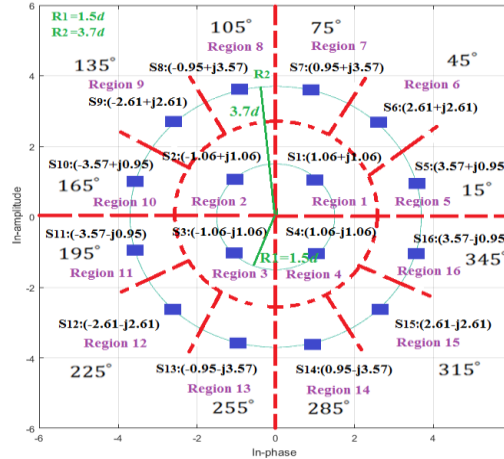


Fig. 3. Proposed signal constellation of coherent 16-APSK.

Based on Fig. 3, we can define all Euclidean distances between two adjacent symbols as a factor of d ; hence, radii R_1 and R_2 are $1.5d$ and $3.7d$ respectively. As a result, all Euclidean distances between symbols of coherent 16-APSK can be defined as Eq.(1). For example, $d_{1,2}$ denotes the Euclidean distance between symbol S_1 and symbol S_2 .

$$\begin{aligned}
 d_{1,2} &= d_{2,3} = d_{3,4} = d_{4,1} = 2.12d; \\
 d_{1,6} &= d_{2,9} = d_{3,12} = d_{4,15} = 2.2d; \\
 d_{1,7} &= d_{1,5} = d_{4,14} = d_{2,10} = d_{2,8} = d_{3,13} = d_{3,11} = d_{4,16} = 2.51d; \\
 d_{5,6} &= d_{6,7} = d_{7,8} = d_{8,9} = d_{9,10} = d_{10,11} = d_{11,12} = d_{12,13} = d_{13,14} = d_{14,15} = d_{15,16} = d_{16,5} = 1.91d.
 \end{aligned} \tag{1}$$

Therefore, by using the union bound of M-ary modulation [7], its symbol error probability (SEP) P_s can be written as

$$P_s = \frac{1}{M} \sum_{w=1}^M \sum_{j \neq 1, j \neq w}^M P(S_w \rightarrow S_j); M = 16, \tag{2}$$

where $P(S_w \rightarrow S_j)$ is the pairwise symbol error probability where symbol S_w can be erroneously decided as symbol S_j . Note that $P(S_w \rightarrow S_j)$ can be expressed using Marcum Q-function [10]; where $d_{w,j}$ is the Euclidean distance between symbol S_w and symbol S_j and it can be selected from Eq.(1). In Eq.(3), N_0 is the two-side of Gaussian noise spectral density. For the simulation of BEP, its value of 10^{-10} watts per hertz (W/Hz) [10] is used in our paper.

$$P(S_w \rightarrow S_j) = Q\left(\frac{d_{w,j}}{\sqrt{2N_0}}\right). \tag{3}$$

For the considered Rayleigh fading channel, one-ray model is discussed first and Eq.(4) denotes the PDF of Rayleigh fading with envelope r [5, 8] where σ is the standard deviation of Rayleigh distribution. Note that r is equal to $\mathcal{A} \cos(\omega t - \theta)$.

$$f(r) = \frac{r}{\sigma^2} e^{-\left(\frac{r^2}{2\sigma^2}\right)}; r > 0. \tag{4}$$

In addition, we also need to know the average symbol energy E_s [9] of coherent 16-APSK and the value is $10.83d^2$ by Eq.(5), where $M=16$ is the total number of symbols; $N_1=4$ and $N_2=12$ are the number of symbols on the inner and outer ring respectively according to Fig. 3.

$$E_s = \frac{1}{M} [(N_1 \times R_1^2) + (N_2 \times R_2^2)] = 10.83d^2 \rightarrow d = 0.303\sqrt{E_s}. \tag{5}$$

Hence, the Euclidean distance of symbol S_1 and symbol S_2 , $2.12d$, can be identical to $0.642\sqrt{E_s}$ by the above equation. As a result, $P(S_1 \rightarrow S_2)$ of symbol S_1 is shown by the first term of pairwise symbol error probability and the total symbol error probability of symbol S_1 can be shown as Eq.(6).

$$\begin{aligned}
 S_1: P(S_1 \rightarrow S_2) &+ P(S_1 \rightarrow S_4) + P(S_1 \rightarrow S_5) + P(S_1 \rightarrow S_6) + P(S_1 \rightarrow S_7) \\
 &= 2Q\left(\frac{0.642\sqrt{E_s}}{\sqrt{2N_0}}\right) + 2Q\left(\frac{0.760\sqrt{E_s}}{\sqrt{2N_0}}\right) + Q\left(\frac{0.666\sqrt{E_s}}{\sqrt{2N_0}}\right). \tag{6}
 \end{aligned}$$

Likewise, all other symbol error probability of the remaining symbols are defined as:

$$\begin{aligned}
S_2: & P(S_2 \rightarrow S_1) + P(S_2 \rightarrow S_3) + P(S_2 \rightarrow S_8) + P(S_2 \rightarrow S_9) + P(S_2 \rightarrow S_{10}) \\
& = 2Q\left(\frac{0.642\sqrt{E_s}}{\sqrt{2N_0}}\right) + 2Q\left(\frac{0.760\sqrt{E_s}}{\sqrt{2N_0}}\right) + Q\left(\frac{0.666\sqrt{E_s}}{\sqrt{2N_0}}\right);
\end{aligned}$$

$$\begin{aligned}
S_3: & P(S_3 \rightarrow S_2) + P(S_3 \rightarrow S_4) + P(S_3 \rightarrow S_{11}) + P(S_3 \rightarrow S_{12}) + P(S_3 \rightarrow S_{13}) \\
& = 2Q\left(\frac{0.642\sqrt{E_s}}{\sqrt{2N_0}}\right) + 2Q\left(\frac{0.760\sqrt{E_s}}{\sqrt{2N_0}}\right) + Q\left(\frac{0.666\sqrt{E_s}}{\sqrt{2N_0}}\right);
\end{aligned}$$

$$\begin{aligned}
S_4: & P(S_4 \rightarrow S_1) + P(S_4 \rightarrow S_3) + P(S_4 \rightarrow S_{14}) + P(S_4 \rightarrow S_{15}) + P(S_4 \rightarrow S_{16}) \\
& = 2Q\left(\frac{0.642\sqrt{E_s}}{\sqrt{2N_0}}\right) + 2Q\left(\frac{0.760\sqrt{E_s}}{\sqrt{2N_0}}\right) + Q\left(\frac{0.666\sqrt{E_s}}{\sqrt{2N_0}}\right);
\end{aligned}$$

$$\begin{aligned}
S_5: & P(S_5 \rightarrow S_1) + P(S_5 \rightarrow S_6) + P(S_5 \rightarrow S_{16}) \\
& = Q\left(\frac{0.760\sqrt{E_s}}{\sqrt{2N_0}}\right) + 2Q\left(\frac{0.578\sqrt{E_s}}{\sqrt{2N_0}}\right);
\end{aligned}$$

$$\begin{aligned}
S_6: & P(S_6 \rightarrow S_1) + P(S_6 \rightarrow S_5) + P(S_6 \rightarrow S_7) \\
& = Q\left(\frac{0.666\sqrt{E_s}}{\sqrt{2N_0}}\right) + 2Q\left(\frac{0.578\sqrt{E_s}}{\sqrt{2N_0}}\right);
\end{aligned}$$

$$\begin{aligned}
S_7: & P(S_7 \rightarrow S_1) + P(S_7 \rightarrow S_6) + P(S_7 \rightarrow S_8) \\
& = Q\left(\frac{0.760\sqrt{E_s}}{\sqrt{2N_0}}\right) + 2Q\left(\frac{0.578\sqrt{E_s}}{\sqrt{2N_0}}\right);
\end{aligned}$$

$$\begin{aligned}
S_8: & P(S_8 \rightarrow S_2) + P(S_8 \rightarrow S_7) + P(S_8 \rightarrow S_9) \\
& = Q\left(\frac{0.760\sqrt{E_s}}{\sqrt{2N_0}}\right) + 2Q\left(\frac{0.578\sqrt{E_s}}{\sqrt{2N_0}}\right);
\end{aligned}$$

$$\begin{aligned}
S_9: & P(S_9 \rightarrow S_2) + P(S_9 \rightarrow S_8) + P(S_9 \rightarrow S_{10}) \\
& = Q\left(\frac{0.666\sqrt{E_s}}{\sqrt{2N_0}}\right) + 2Q\left(\frac{0.578\sqrt{E_s}}{\sqrt{2N_0}}\right);
\end{aligned}$$

$$\begin{aligned}
S_{10}: & P(S_{10} \rightarrow S_2) + P(S_{10} \rightarrow S_9) + P(S_{10} \rightarrow S_{11}) \\
& = Q\left(\frac{0.760\sqrt{E_s}}{\sqrt{2N_0}}\right) + 2Q\left(\frac{0.578\sqrt{E_s}}{\sqrt{2N_0}}\right);
\end{aligned}$$

$$\begin{aligned}
S_{11}: & P(S_{11} \rightarrow S_3) + P(S_{11} \rightarrow S_{10}) + P(S_{11} \rightarrow S_{12}) \\
& = Q\left(\frac{0.760\sqrt{E_s}}{\sqrt{2N_0}}\right) + 2Q\left(\frac{0.578\sqrt{E_s}}{\sqrt{2N_0}}\right);
\end{aligned}$$

$$S_{12}: P(S_{12} \rightarrow S_3) + P(S_{12} \rightarrow S_{11}) + P(S_{12} \rightarrow S_{13})$$

$$= Q\left(\frac{0.666\sqrt{E_s}}{\sqrt{2N_0}}\right) + 2Q\left(\frac{0.578\sqrt{E_s}}{\sqrt{2N_0}}\right);$$

$$S_{13}: P(S_{13} \rightarrow S_3) + P(S_{13} \rightarrow S_{12}) + P(S_{13} \rightarrow S_{14}) \\ = Q\left(\frac{0.760\sqrt{E_s}}{\sqrt{2N_0}}\right) + 2Q\left(\frac{0.578\sqrt{E_s}}{\sqrt{2N_0}}\right);$$

$$S_{14}: P(S_{14} \rightarrow S_4) + P(S_{14} \rightarrow S_{13}) + P(S_{14} \rightarrow S_{15}) \\ = Q\left(\frac{0.760\sqrt{E_s}}{\sqrt{2N_0}}\right) + 2Q\left(\frac{0.578\sqrt{E_s}}{\sqrt{2N_0}}\right);$$

$$S_{15}: P(S_{15} \rightarrow S_4) + P(S_{15} \rightarrow S_{14}) + P(S_{15} \rightarrow S_{16}) \\ = Q\left(\frac{0.666\sqrt{E_s}}{\sqrt{2N_0}}\right) + 2Q\left(\frac{0.578\sqrt{E_s}}{\sqrt{2N_0}}\right);$$

$$S_{16}: P(S_{16} \rightarrow S_4) + P(S_{16} \rightarrow S_5) + P(S_{16} \rightarrow S_{15}) \\ = Q\left(\frac{0.760\sqrt{E_s}}{\sqrt{2N_0}}\right) + 2Q\left(\frac{0.578\sqrt{E_s}}{\sqrt{2N_0}}\right).$$

(7)

Furthermore, the overall average symbol error probability P_s can be defined as

$$P_s = \frac{1}{16}(S_1 + S_2 + S_3 + S_4 + S_5 + S_6 + S_7 + S_8 + S_9 + S_{10} + S_{11} + S_{12} + S_{13} + S_{14} + S_{15} + S_{16}). \\ = \frac{1}{16} \left[8Q\left(\frac{0.642\sqrt{E_s}}{\sqrt{2N_0}}\right) + 16Q\left(\frac{0.760\sqrt{E_s}}{\sqrt{2N_0}}\right) + 8Q\left(\frac{0.666\sqrt{E_s}}{\sqrt{2N_0}}\right) + 24Q\left(\frac{0.578\sqrt{E_s}}{\sqrt{2N_0}}\right) \right]. \quad (8)$$

In addition, assuming all symbol errors are equally probable [10], the relationship between P_s and the bit error probability $P_{b,16\text{-APSK,AWGN}}$ of the un-coded coherent 16-APSK can be defined as Eq.(9) over AWGN, where $M=2^k$ and $k=4$ is the number of bits per symbol. Note that $P_{b,16\text{-APSK,AWGN}}$ is defined with conventional ratio of bit energy to noise power spectral density ratio E_b/N_0 .

$$P_{b,16\text{-APSK,AWGN}} = \left(\frac{M}{2}\right) P_s = \frac{8}{15} \left\{ \frac{1}{16} \left[8Q\left(\frac{0.642\sqrt{E_b}}{\sqrt{2N_0}}\right) + 16Q\left(\frac{0.760\sqrt{E_b}}{\sqrt{2N_0}}\right) + 8Q\left(\frac{0.666\sqrt{E_b}}{\sqrt{2N_0}}\right) + 24Q\left(\frac{0.578\sqrt{E_b}}{\sqrt{2N_0}}\right) \right] \right\}. \quad (9)$$

Then the un-coded bit error probability (BEP) [11] of coherently detected 16-APSK using one-ray Rayleigh fading channel model can be defined by using Eq. (9) of $P_{b,16\text{-APSK,AWGN}}$ and Eq.(4) of variables as

$$P_{b,16\text{-APSK,Rayleigh}} = \int_0^\infty (P_{b,16\text{-APSK,AWGN}}) \times \left(\frac{r}{\sigma^2}\right) e^{-\left(\frac{r^2}{2\sigma^2}\right)} dr. \quad (10)$$

The BEP performance of the proposed un-coded coherent 16-APSK over AWGN and one-ray Rayleigh fading channel is shown in Fig. 4. We can see that there is a tiny gap between the simulated and theoretical BEPs for both channels considered due to the inter-symbol interference (ISI) [24]. Furthermore, the proposed coherent 16-APSK needs more transmission power over one-ray Rayleigh fading channel when it is compared with the case of over AWGN for a fixed BEP. For example, as the simulation results show, the proposed coherent 16-APSK system requires about 5-7 dB more power to achieve the desirable BEP of 10^{-3} over one-ray Rayleigh fading channel, compared to the case over AWGN. Note that the simulated BEP is obtained by using Monte Carlo simulation [12].

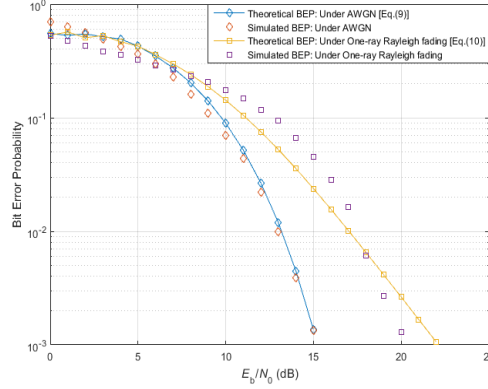


Fig. 4. BEP performance of the proposed un-coded coherent 16-APSK over the considered channel.

4. Regular LDPC Code

In general, advantages of regular LDPC code can be summarized as following: (a) Suitable for parallel implementation, (b) More amenable to high coding rate, (c) Lower error floor, and (d) Superior error correcting capability. In this paper, the proposed regular LDPC code is one kind of linear block code (LBC) in which each code-word U is equal to the product of the transmitted message m and the generator matrix G as in Eq.(11) [14].

$$U = [m_1 m_2 m_3 \dots m_k] \begin{bmatrix} g_{1,1} & \dots & g_{1,n} \\ \vdots & \ddots & \vdots \\ g_{k,1} & \dots & g_{k,n} \end{bmatrix} = m \cdot G. \quad (11)$$

Wherein, the generator matrix G of the systematic is usually a $k \times n$ matrix (n is larger than k) as Eq.(12).

$$G = \begin{bmatrix} p_{1,1} & \dots & p_{1,n-k} & 1 & \dots & 0 \\ \vdots & \ddots & \vdots & \vdots & \ddots & \vdots \\ p_{k,1} & \dots & p_{k,n-k} & 0 & \dots & 1 \end{bmatrix} = [P_{k \times (n-k)} | I_{k \times k}]_{k \times n}. \quad (12)$$

By Eq.(12), the parity check matrix H can be defined as

$$H = [I_{(n-k) \times (n-k)} | P_{k \times (n-k)}^T] = [I_{(n-k) \times (n-k)} | P_{(n-k) \times k}]_{(n-k) \times n}. \quad (13)$$

The parity-check matrix $H_{(n-k) \times n}$ used in the decoding of regular LDPC code is shown in Eq.(14). This decoder can decode each bit simultaneously rather than Meggitt decoder [30] of conventional code. Note that n and k are 14 and 6 respectively. As a regular LDPC code, each column and row has the same number of '1' respectively.

$$H_{(n-k) \times n} = \begin{bmatrix} 1 & 0 & 1 & 0 & 1 & 0 & 1 & 0 & 1 & 0 & 1 & 0 & 1 & 0 \\ 0 & 1 & 0 & 1 & 0 & 1 & 0 & 1 & 0 & 1 & 0 & 1 & 0 & 1 \\ 1 & 0 & 1 & 0 & 1 & 0 & 1 & 0 & 1 & 0 & 1 & 0 & 1 & 0 \\ 0 & 1 & 0 & 1 & 0 & 1 & 0 & 1 & 0 & 1 & 0 & 1 & 0 & 1 \\ 1 & 0 & 1 & 0 & 1 & 0 & 1 & 0 & 1 & 0 & 1 & 0 & 1 & 0 \\ 0 & 1 & 0 & 1 & 0 & 1 & 0 & 1 & 0 & 1 & 0 & 1 & 0 & 1 \\ 1 & 0 & 1 & 0 & 1 & 0 & 1 & 0 & 1 & 0 & 1 & 0 & 1 & 0 \\ 0 & 1 & 0 & 1 & 0 & 1 & 0 & 1 & 0 & 1 & 0 & 1 & 0 & 1 \end{bmatrix}_{8 \times 14}. \quad (14)$$

This parity check matrix $H_{8 \times 14}$ has eight rows and fourteen columns so we have 8 parity check nodes for error correction and 14 information bit nodes for storage information (or code-word U) in the decoder. It should be noticed that the parity check node connects with the information bit node by the number of '1'; otherwise, they do not connect with each other by the number of '0'. To decode the message m , each information bit node transmits each code-word U to all adjacent parity check nodes for decoding equally. Next, each parity check node transmitted decoded code-word U back to all adjacent information bit nodes equally. Finally, repeat these two steps to construct each iterative decoding until having the perfect received message m .

Mathematically, this received message m can be expressed by log-likelihood ratio (LLR) [9] [18] [22] over AWGN as in Eq.(15). $P(y|m)$ is the conditional pdf of the received signal, y , conditioned on the transmitted message m (bit 1 or bit 0). If $L(y)$ is larger than decision threshold of LLR calculation, the received message m is decoded as bit 1. Otherwise, bit 0 is assumed. Q is the number of iteration and the value is 2; it means that each code-word U completes two round trips between information bit nodes and parity check nodes for decoding.

$$L(y)_{Coded\ 16-APSK,AWGN} = \sum_{l=0}^Q (\log \frac{P(y|m=1)}{P(y|m=0)})_l. (15)$$

Considering the effect of Rayleigh fading [20-21], the corresponding BEP can be expressed by using $L(y)_{Coded\ 16-APSK,AWGN}$ and Eq.(4) of parameter r as

$$P_{b,Coded\ 16-APSK, Rayleigh} = \int_0^\infty [L(y)_{Coded\ 16-APSK,AWGN}] \times (\frac{r}{\sigma^2} e^{-\frac{r^2}{2\sigma^2}}) dr. (16)$$

The theoretical BEP of the proposed regular LDPC coded coherent 16-APSK system is illustrated in Fig. 5. In comparison with Fig. 4 of the un-coded case, at BEP of 10^{-3} , we get coding gain of 3 dB (under AWGN) and 7-9 dB under fading (with one-ray model) respectively. At the BEP of 10^{-6} , the proposed coded system required 20 dB of E_b/N_0 under one-ray Rayleigh fading channel, while it needs 16 dB of E_b/N_0 under AWGN. In other words, with the help of regular LDPC code, the proposed coherent 16-APSK can approach closely to the lower BEP under AWGN at the same power constraint compared to one-ray Rayleigh channel, implying that the effect of fading in one-ray Rayleigh channel can be minimized considerably thereby. For example, the system can reach the BEP of 10^{-6} under AWGN at 16 dB but the BEP of one-ray Rayleigh channel is only lower than 10^{-4} slightly at the identical transmission power. The main reason is that the signal of one-ray Rayleigh channel may not have perfect ground reflection due to object 1 in Fig. 1; the transmission power of reflected ray is expected to be reduced that compared with transmitted ray. In Fig. 5, we do not show the simulated BEP curve for the regular LDPC coded case due to the higher complexity in the design of regular LDPC code. However, the theoretical BEP shown in Fig. 5 using Eq.(15) and Eq.(16) are often referred to as the upper bound of the BEP performance [24].

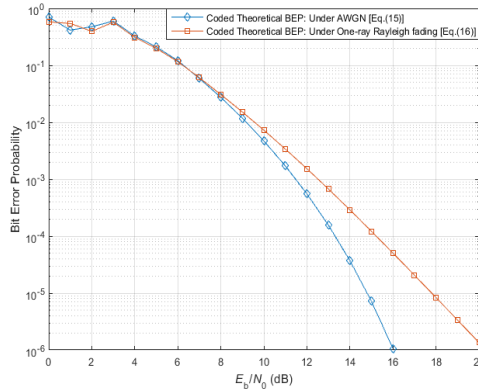


Fig. 5. Theoretical BEP curves of proposed regular LDPC coded coherent 16-APSK in AWGN and one-ray Rayleigh channel.

5. Delay Spread

If the delay spread occurs in the considered Rayleigh fading channel, each transmitted signal goes through different signal paths between the transmitter and the receiver. As a result, the time of arrival for each path of the transmitted signal is different at the receiver. The probability density function (PDF) of delay spread of two successive transmitted signals is defined as the exponential distribution $p(t)$ together with the delay spread τ_d and the average delay spread τ_m in Eq.(17) [13]. Note that all parameters are in [sec].

$$p(t) = \frac{1}{\tau_m} e^{-\frac{t}{\tau_m}};$$

$$\tau_d = \sqrt{\int_0^\infty (t - \tau_m)^2 p(t) dt}. (17)$$

Due to the input binary data sequence, the E_b [17] of delay spread τ_d can be interpreted as Eq.(18) where T is bit duration and assumed to be much greater than τ_d . Under the consideration of reflected ray $A \cos(\omega t - \theta)$, θ is equal to $\omega \tau_d$ but it is very closed to 0° .

$$E_b = \int_0^T [A \cos(\omega t - \omega \tau_d)]^2 dt = [A \cos(\omega t - \omega \tau_d)]^2 T = [A \cos(2\pi f(t - \tau_d))]^2 T. \quad (18)$$

If we apply Eq.(18) to Eq.(10), the un-coded BEP of coherent 16-APSK under the effect of delay spread in one-ray Rayleigh fading channel is shown below. Note that $P_{b,16\text{-APSK},\text{AWGN}}$ is from Eq.(9) where r is the envelope of Rayleigh faded signals and E_b is from Eq.(18).

$$P_{b,16\text{-APSK},\text{Rayleigh},h,\text{delayspread}} = \int_0^\infty (P_{b,16\text{-APSK},\text{AWGN}}) \times \left(\frac{r}{\sigma^2} e^{-\frac{r^2}{2\sigma^2}}\right) dr; E_b = [A \cos(2\pi f(t - \tau_d))]^2 T. \quad (19)$$

In this paper, the considered parameters of the effect of delay spread for 2.5 GHz indoor wireless communication system are:

- The average delay spread τ_m is defined as 3.52×10^{-9} [sec] [1].
- The calculation of delay spread τ_d is derived as 1.61×10^{-17} [sec] from Eq.(17) based on (a) and compared with 2×10^{-8} [sec] from [1].
- The center frequency f is selected as 2.5 GHz from [1].

6. Computer Simulations

6.1 Un-coded BEP of Coherent 16-APSK with Delay Spread using One-ray Model

The effect of delay spread on the BEP performance of the un-coded coherent 16-APSK is shown in Fig. 6. We can observe that the effect of delay spread is not significant in one-ray Rayleigh fading channel due to the nature of very small value in practical 2.5 GHz indoor wireless delay spread measurement [1] and this simulation result is very close to the result of [11]. However, the ISI and scattered signals still affect the BEP performance of the system resulting the gap between simulated and theoretical BEP curves of the cases, with or without delay spread [24]. As a result, we can conclude that the effect of delay spread is negligible in our considered channel compared to the effect of ISI and scattering signal. Note that the reflected ray of amplitude \mathcal{A} is 0.5 from Section 2 and the bit duration T is 10^{-3} [sec] [17] with the E_b of delay spread from Eq.(18).

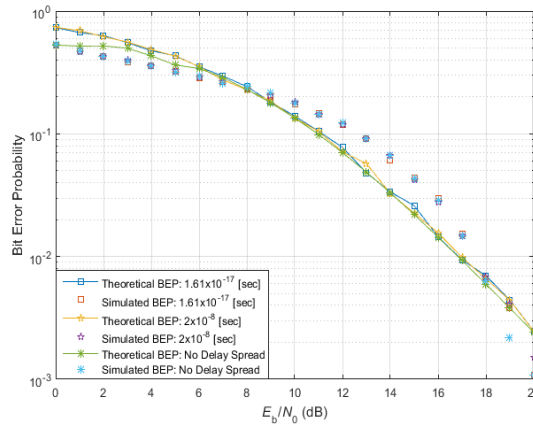


Fig. 6. BEP curves of un-coded coherent 16-APSK with different delay spread under one-ray model (Center frequency $f = 2.5$ GHz).

6.2 BEP Performance of Un-coded and Coded Coherent 16-APSK System without Delay Spread Using One-ray and Four-ray Fading Model

According to results of Section 4, regular LDPC code with its coding gain is very effective in reducing the effect of fading in one-ray Rayleigh fading channel. Since one-ray fading model we used may not properly reflect the practical fading channel, we increase the number of rays to 4 and tested the proposed coded system. The theoretical BEP performance of the proposed system using four-ray Rayleigh fading channel is illustrated in Fig. 7 for further discussion. From Fig. 7 (a), for the BEP of 10^{-4} , we can observe that the coded BEP curve in Rayleigh fading channel (one-ray) moves closely to that of AWGN, which means that the effect of fading has been considerably minimized with the employment of regular LDPC code.

Whereas, in the un-coded case, the BEP curve in Rayleigh fading channel (one-ray) moves away from that of AWGN significantly on account of the fading effect. In other words, regular LDPC code can effectively compensate the effect of channel fading. By the result, the coded system under fading yields the almost identical BEP performance in AWGN and Rayleigh fading channel. Last but not least, the channel scenario of Fig. 7 (a) also can be extended to four-ray Rayleigh fading channel in Fig. 7 (b). We can observe that coded four-ray Rayleigh fading (Fig. 7 (b)) needs only 8 dB to approach BEP of 10^{-4} but coded Rayleigh fading (Fig. 7(a)) requires 15 dB to arrive the same BEP. This simulation result can be explained by central-limit theorem [32]. This theory indicates that the probability density function of a sum of N independent random variables tends to approach a Gaussian distribution as the number N increases; furthermore, it also applied even when each of individual random variables N is not Gaussian distribution, such as Eq.(4). Once the sum of N independent random variables approaches a better Gaussian distribution by larger N , received data can be detected by higher correct detection probabilities and in terms of lower BEP by Marcum Q-function of Eq. (3) at the identical E_b/N_0 .

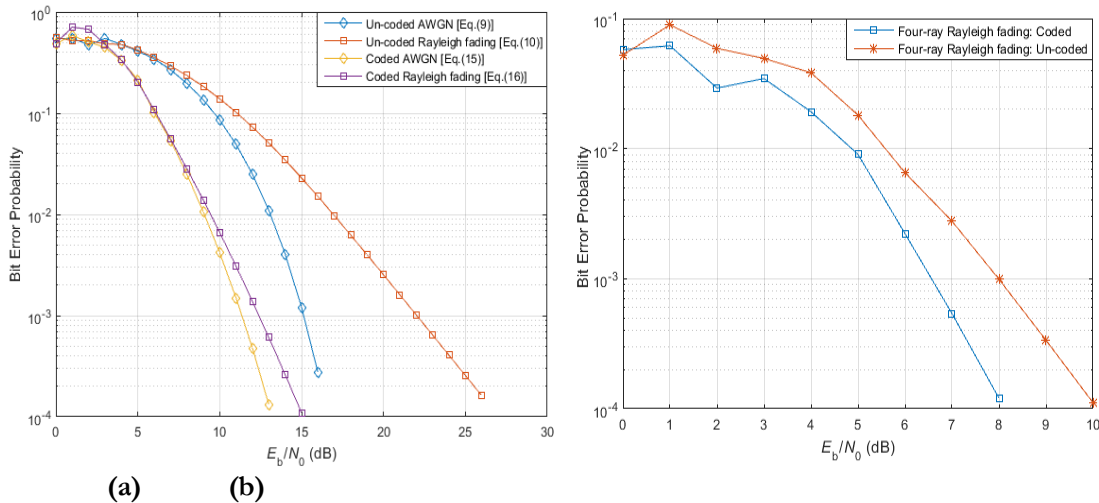


Fig. 7.Theoretical BEPs comparison between un-coded and coded coherent 16-APSK in (a) one-ray Rayleigh fading channel and (b) four-ray Rayleigh fading channel without delay spread.

6.3 BEP Performance of Coded Coherent 16-APSK with Delay Spread of 2×10^{-8} [sec] and Center Frequency of 2.5 GHz under One-ray Model, Three-ray model and Four-ray model

In the previous section, it was shown that under one-ray fading model, the effect of delay spread is negligible (using 2.5 GHz of center frequency) comparing the adverse effects of ISI and scattering toward BEP performance of the proposed scheme. Now it is valuable to check the effect of delay spread under the more practical multi-ray fading model. Based on [19], assuming signal paths are independent, Rayleigh distribution of three-ray model and four-ray fading model can be written as below and each r can be represented by reflected ray $A \cos(\omega t - \theta)$ with different $A = 0.5, 0.33, 0.66$ and 0.85 and $\theta = 0^\circ$ under $f = 2.5\text{GHz}$.

$$f(r_1, r_2, r_3) = \frac{r_1 r_2 r_3}{\sigma_1^2 \sigma_2^2 \sigma_3^2} e^{-\left(\frac{r_1^2 r_2^2 r_3^2}{8\sigma_1^2 \sigma_2^2 \sigma_3^2}\right)} ; r_1, r_2, r_3 > 0; (Three - ray)$$

$$f(r_1, r_2, r_3, r_4) = \frac{r_1 r_2 r_3 r_4}{\sigma_1^2 \sigma_2^2 \sigma_3^2 \sigma_4^2} e^{-\left(\frac{r_1^2 r_2^2 r_3^2 r_4^2}{16\sigma_1^2 \sigma_2^2 \sigma_3^2 \sigma_4^2}\right)} ; r_1, r_2, r_3, r_4 > 0. (Four - ray) (20)$$

Fig. 8 shows the theoretical BEP performance of coded coherent 16-APSK system under one-ray, three-ray, four-ray Rayleigh fading models and AWGN channel. According to Fig. 6 and [11], the effect of delay spread is independent on our proposed system so we can define all models with the same delay spread: 2×10^{-8} [sec].

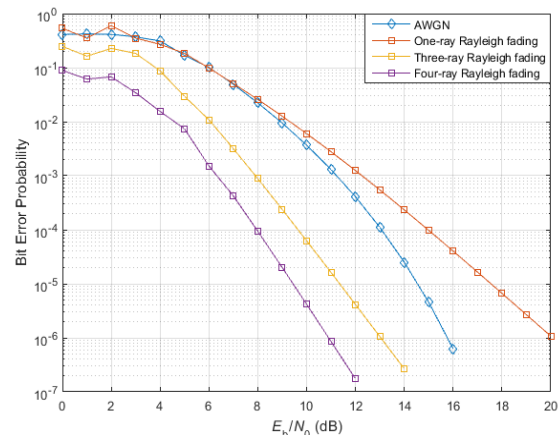


Fig. 8. Theoretical BEPs of coded coherent 16-APSK with delay spread of 2×10^{-8} [sec] using one-ray model, three-ray model and four-ray Rayleigh fading model.

As the theoretical simulation results shown that, for the BEP of 10^{-6} , it requires less power in three-ray and four-ray Rayleigh fading channel, whereas it needs more power in one-ray Rayleigh fading channel, when compared with case of AWGN channel. In other words, if Rayleigh fading channel is modeled as multiple-ray model (than one-ray), that is close to the practical indoor fading channel; this reasonable result is similar to the results found in [23] without extra bandwidth requirement and can also be proven by central-limit theorem.

7. Conclusion

In this work, we propose a coherently detected regular LDPC coded 16-APSK as a possible candidate for the wireless indoor communication scheme under the adverse effects of Rayleigh fading. Analytic BEP performance of the proposed scheme as well as the simulation results under multi-ray (up to four rays) model of indoor Rayleigh fading confirm the effectiveness of the regular LDPC FEC coding by yielding sufficient coding gain to ensure the reasonable error performance under AWGN as well as fading. Additional analysis under the delay spread confirms that, at 2.5 GHz center frequency, effect of delay spread is negligible and insignificant towards desired BEP due to sufficient coding gain under fading effect. Changing the fading model from one ray to more practical 4-ray actually enhances the BEP performance of the proposed scheme due to the higher correct detection probabilities by central-limit theorem.

References

- Yuanita, R. I., Hendratoro, G., & Lin, D.-B. (2018). Multipath delay spread measurement for indoor wireless device-to-device communications. Proceedings of the 3rd International Conference on Intelligent Green Building and Smart Grid: Yi-Lan, Taiwan.
- Abudoukeremu, A., Ida, Y., Matsumoto, T., & Matsufuji, S. (2018). Multicarrier transmission systems with spreading sequences in large delay spread channel. Proceedings of the 6th International Workshop on Signal Design and its Applications in Communications: Tokyo, Japan.
- Richardson, T. J., Urbanke, R. (2001). The capacity of low-density parity-check codes under message-passing decoding. *IEEE Transactions on Information Theory*, 47(2), 599–618.
- Baldi, M., Chiaraluce, F., Angelis, A., Marchesani, R., Schillaci, S. (2012). A comparison between APSK and QAM in wireless tactical scenarios for land mobile systems. *EURASIP Journal on Wireless Communications and Networking*.
- Peebles, P. (2001). Probability, Random Variables and Random Signal Principles (4thed.). New York: McGraw-Hill.
- Sebesta, J. (2009). Efficient method for APSK demodulation. Proceedings of the 3th International Conference on Applied Mathematics, Simulation, Modeling, Circuits, Systems and Signals: Athens, Greece.
- Sung, W., Kang, S., Kim, P., Chang, D.-I., Shin, D.-J., (2009). Performance analysis of APSK modulation for DVB-S2 transmission over nonlinear channels. *International Journal of Satellite Communications*, 27, 295–311.
- Proakis, J. G., Salehi, M., & Bauch, G. (2013). Modern Communication Systems Using Matlab. Connecticut: Cengage Learning.
- Lin, S., & Costello, D. J. (2004). Error Control Coding (2nded.). New Jersey: Pearson-Prentice Hall.

- Haykin, S. (1988). *Digital Communications*. New York: Wiley.
- Xia, Y., Tse, C., Lau, F., (2004). Performance of differential chaos-shift-keying digital communication systems over a multipath fading channel with delay spread. *IEEE Transactions on Circuits and Systems-II: Express Briefs*, 51(12), 680–684.
- Zhan, J., Wang, L., Katz, M., Chen, G., (2017). A differential chaotic bit-interleaved coded modulation system over multipath Rayleigh channels. *IEEE Transactions on Communications*, 65(12), 5257–5265.
- Agrawal, D.-P., & Zeng, Q.-A. (2016). *Introduction to Wireless and Mobile Systems (4thed.)*. Massachusetts: Cengage Learning.
- Jiang, Y. (2010). *A Practical Guide to Error-Control Coding Using Matlab*. Massachusetts: Artech House.
- Buzzi, S., Venturino, L., Zappone, A., (2010). Multipath delay acquisition in asynchronous doubly-selective DS/CDMA fading channels. *IEEE Communications Letters*, 14(4), 276–278.
- Buzzi, S., Massaro, V., (2008). Parameter estimation and multiuser detection for bandlimited long-code CDMA systems. *IEEE Transactions on Wireless Communications*, 7(6), 2307–2317.
- Ziener, R., & Tranter, W. (1995). *Principles of Communications: Systems, Modulation, and Noise (4thed.)*. Massachusetts: Houghton Mifflin.
- Chung, S.-Y., Richardson, T. J., Urbanke, R. L., (2001). Analysis of sum-product decoding of low-density parity-check codes using a Gaussian approximation. *IEEE Transactions on Information Theory*, 47(2), 657–670.
- Dimitrakopoulos, G. A., Capsalis, C. N., (2000). Statistical modeling of rms-delay spread under multipath fading conditions in local areas. *IEEE Transactions on Vehicular Technology*, 49(5), 1522–1528.
- Hou, J., Siegel, P., Milstein, L., (2001). Performance analysis and code optimization of low density parity-check codes on Rayleigh fading channels. *IEEE Journal on Selected Areas in Communications*, 19(5), 924–934.
- Kaddoum, G., Richardson, F., Gagnon, F., (2013). Design and analysis of a multi-carrier differential chaos shift keying communication system. *IEEE Transactions on Communications*, 61(8), 3281–3291.
- Lehmann, F., Maggio, G., (2003). Analysis of the iterative decoding of LDPC and product codes using the Gaussian approximation. *IEEE Transactions on Information Theory*, 49(11), 2993–3000.
- Bargallo, J., Roberts, J., (1995). Performance of BPSK and TCM using the exponential multipath profile model for spread-spectrum indoor radio channels. *IEEE Transactions on Communications*, 43(2/3/4), 615–623.
- Wang, L., Cai, G., Chen, G., (2015). Design and performance analysis of a new multiresolution M-ary differential chaos shift keying communication system. *IEEE Transactions on Wireless Communications*, 14(9), 5197–5208.
- Shafi, M., (1987). Statistical analysis/simulation of a three ray model for multipath fading with applications to outage prediction. *IEEE Journal on Selected Areas in Communications*, Sac-5(3), 389–401.
- Sakagami, S., Hosoya, Y., (1982). Some experimental results on in-band amplitude dispersion and a method for estimating in-band linear amplitude dispersion. *IEEE Transactions on Communications*, 30(8), 1875–1888.
- Shafi, M., (1988). Influence of terrain-induced reflections on the performance of high-capacity digital radio systems. *IEEE Transactions on Communications*, 36(3), 245–251.
- McClaning, K. (2012). *Wireless Receiver Design for Digital Communications*. North Carolina: Scitech.
- Laughton, D., Bocchetta, M. A., King, C. R., & Free, C. E. (1993). The effects on spread spectrum signals of multipath fading in an indoor environment. Proceedings of the IEE Colloquium on ‘Spread Spectrum Techniques for Radio Communication Systems’: London, United Kingdom.
- Meggitt, J., (1961). Error correcting codes and their implementation for data transmission systems. *IRE Transactions on Information Theory*, 7(4), 234–244.
- Chayratsami, P., & Thuaykaew, S. (2014). The optimum ring ratio of 16-APSK in LTE uplink over nonlinear system. Proceedings of the 16th International Conference on Advanced Communication Technology: Pyeongchang, South Korea.
- Taub, H., & Schilling, D. L. (1971). *Principles of Communication Systems*. New York: McGraw-Hill.
- Pedrotti, F. L., Pedrotti, L. M., & Pedrotti, L. S. (2018). *Introduction to Optics*. United Kingdom: Cambridge.